*submitted to BIOPHYSICAL JOURNAL (REGULAR ARTICLE)*

# Supporting Material

# Rates and stoichiometries of metal ion probes of cysteine residues within ion channels

Lai-Sheung Choi, Tivadar Mach and Hagan Bayley[1]

Department of Chemistry, University of Oxford, Oxford, OX1 3TA, United Kingdom

[1] To whom correspondence should be addressed. Address: Department of Chemistry, University of Oxford, Oxford, OX1 3TA, United Kingdom. Phone: +44 1865 285101. Fax: +44 1865 275708. E-mail: hagan.bayley@chem.ox.ac.uk

# SUPPORTING MATERIAL

## 1. Properties of the αHL AG mutant

By contrast with the weak anion selectivity of $(WT)_7$, $(AG)_7$ is cation-selective (the charge selectivity ratio $P_{K^+}/P_{Cl^-}$ is 0.54 for $(WT)_7$ and 3.12 for $(AG)_7$ in 100 mM KCl (*cis*)/ 1 M KCl (*trans*), pH 7.4). The conductance of $(AG)_7$ (2.73 ± 0.01 nS in 2 M KCl, –50 mV) is about 1.5 times higher than that of $(WT)_7$ (1.78 ± 0.01 nS). AG shows comparable hemolytic activity to WT αHL.

## 2. Additional information on the complete blockade of $P_C$ produced by $Ag^+$ ion

To determine whether the full blockade of $P_C$ (see Fig. 4) arises from $Ag^+$-thiol polymer formation, we tried to remove residual thiol from the protein preparation. Thiols, including thioglycolate, β-mercaptoethanol and DTT, were added to provide a reducing environment during protein preparation and for protein storage. Tens of nM of thiols remained in the chamber during planar lipid bilayer experiments. Buffer replacement in the bilayer apparatus was performed in attempts to reduce the thiols to pM concentrations, but pore blockade still occurred soon after $Ag^+$ addition. Replacing the thiols with tris(2-carboxylethyl)phosphine (TCEP) yielded $P_C$ with an unreactive cysteine thiol.

We tested $Ag^+$-thiol polymer formation by the addition of different thiols to $P_C$ in the presence of $Ag^+$. L-Cysteine, cysteamine and thioglycolate caused stepwise current reductions (Fig. S1) similar to the $Ag^+$-induced blockade shown in Fig. 4. The blockade began from the single Ag(I)-bound state ($P_C$-S-Ag), no matter which thiol was used. This reflects the role of $Ag^+$ in initiating polymer formation.

Other metal ions, for example $Cd^{2+}$, $Ni^{2+}$, $Pb^{2+}$ and $Hg^{2+}$, do not cause a full blockade of $P_C$. Colloidal silver ($Ag^0$) formation by light-driven reduction (1) was avoided by keeping the bilayer chamber in the dark. The thiol compounds used also do not reduce $Ag^+$ ion. High quality reagents obtained from two suppliers were used to exclude impurities as a possible source of blockade.

Taking together the experimental findings presented in the main text [1. the unblocking of the pore by the addition of excess thiol (>1 equivalent of thiol relative to the total $AgNO_3$ added; 2. the shorter lag time for blocking in

the presence of added thiol (~100 nM, which is similar to the amount of free $Ag^+$); and, 3. the absence of blockade with the cysteine-free αHL $(AG)_7$ pore], we believe that the blockade of $P_C$ is caused by $Ag^+$-thiol polymer formation initiated at the cysteine thiol group in the lumen of the pore (Fig. S2). Such polymer formation is expected to be very sensitive to trace amounts of thiols present in solution (2–5).

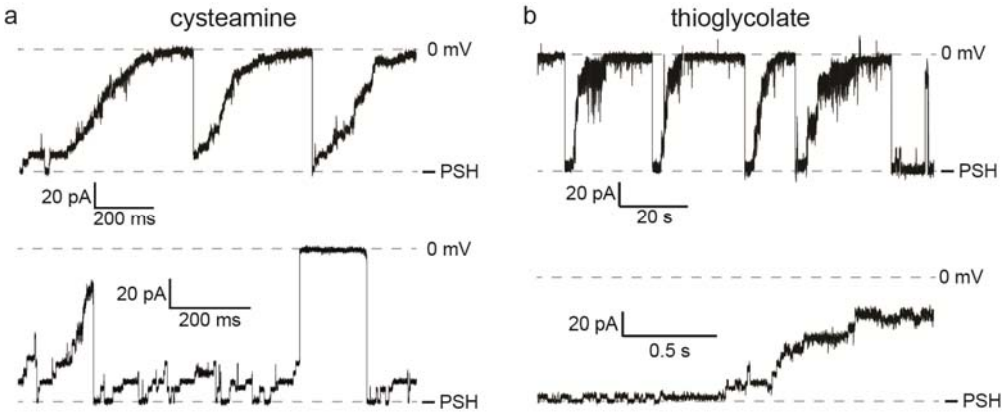


**Figure S1.** Silver(I)-thiol polymer formation in $P_C$. (*A*) Stepwise polymer formation with cysteamine. The two traces were collected under the same conditions. They show the stepwise build-up of different lengths of polymer that lead to different extents of pore blockade. The polymers always break in a single step, presumably by cleavage of the polymer chain near the cysteine residue of the pore (see Fig. S2). Conditions: 133 nM free $Ag^+$ (cis)/16 μM cysteamine (trans). (*B*) Stepwise polymer formation with thioglycolate. The lower trace shows a region of the upper trace with an expanded time axis. As in (*A*), polymers of different lengths were observed. Conditions: 266 nM free $Ag^+$ (cis)/1 μM thioglycolate (trans). L-Cysteine produces current blockades similar to those of thioglycolate. Irreversible pore blockade is observed in the absence of added thiol (see Fig. 4 in the main text). By contrast, the reversible blockades in (*A*) and (*B*) arise from the much higher concentration of thiol present, which promote polymer breakdown.

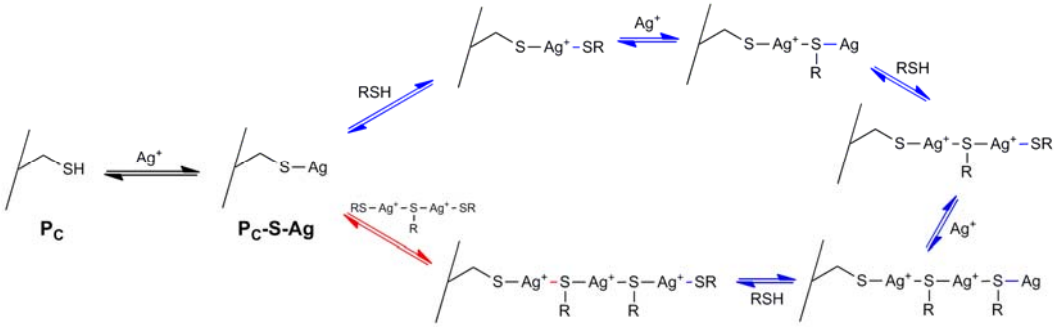


**Figure S2.** Proposed mechanisms for the growth and breakdown of silver(I)-thiol polymer on $P_C$. The alternating addition (or dissociation) of $Ag^+$ ion and thiol molecules (RSH) (black and blue arrows) leads to stepwise polymer growth (or breakdown). Sometimes the silver(I)-thiol polymer is preformed in solution. Its attachment (red arrow) leads to a one-step blockade as seen in Fig. 4*A* in the main text. One-step dissociation of the silver(I)-thiol polymer can also occur, and might be assisted by free thiol molecules. For simplicity, silver-thiol oligomers containing up to three $Ag^+$ ions are drawn. Longer polymers are possible. In addition to the thiol sulfur atom, carboxyl or amino group from the thiol compound can also coordinate to silver(I).

### 3. Binding of $Cd^{2+}$ ion by $P_{CC}$

Our experimental results summarized in Table 1 in the main text show that 1) $P_{CC}$ and $P_C$ have similar $Cd^{2+}$ association rate constants, while 2) the dissociation rate constant of $P_{CC}$ is 370-times lower than that of $P_C$. The $Cd^{2+}$ binding events displayed in Fig. 7*A* must be contributed by the species shown in the box in the following kinetic scheme. Because there is only one current level with $Cd^{2+}$ bound, we suggest that it represents 2, which is implicit in the analysis that follows.

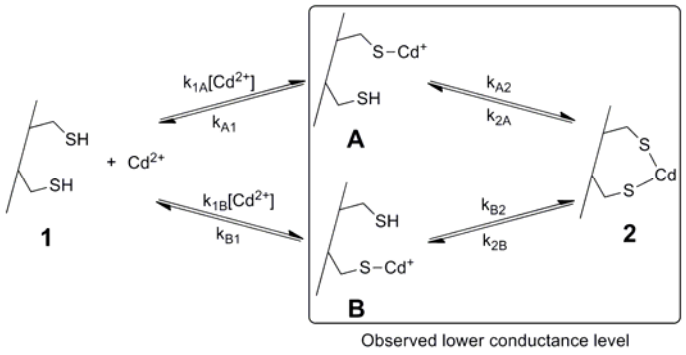


The probabilities of existence for each of the three species in the box are (6):

$$p_2 = \frac{k_{A2}k_{B2}}{k_{A2}k_{B2} + k_{2A}k_{B2} + k_{A2}k_{2B}} \quad \text{..... [1]}$$

$$p_A = \frac{k_{2A}k_{B2}}{k_{A2}k_{B2} + k_{2A}k_{B2} + k_{A2}k_{2B}} \quad \text{..... [2]}$$

$$p_B = \frac{k_{A2}k_{2B}}{k_{A2}k_{B2} + k_{2A}k_{B2} + k_{A2}k_{2B}} \quad \text{..... [3]}$$

where $p_2 + p_A + p_B = 1$

The apparent $Cd^{2+}$ dissociation rate constant $k^{app}_{CC,10}$ (Table 1 in the main text) is:

$$k^{app}_{CC,10} = k_{A1}p_A + k_{B1}p_B$$

and substituting Eq. 2 and Eq. 3:

$$k_{CC,10}^{app} = \frac{k_{A1}k_{2A}k_{B2} + k_{B1}k_{A2}k_{2B}}{k_{A2}k_{B2} + k_{2A}k_{B2} + k_{A2}k_{2B}} \quad \text{..... [4]}$$

Therefore, the mean lifetime in the box is:

$$\left(\overline{\tau_2}\right) = \frac{k_{A2}k_{B2} + k_{2A}k_{B2} + k_{A2}k_{2B}}{k_{A1}k_{2A}k_{B2} + k_{B1}k_{A2}k_{2B}} \quad \text{..... [5]}$$

The lifetime outside the box is:

$$\left(\overline{\tau_1}\right) = \frac{1}{\left(\left(k_{1A} + k_{1B}\right)\left[Cd^{2+}\right]\right)} = \frac{1}{\left(k_{CC,01}^{app}\left[Cd^{2+}\right]\right)} \quad \text{..... [6]}$$

where $k^{app}_{CC,01}$ is the apparent association rate constant (Table 1).

If we assume that the two cysteine thiol groups have the same association and dissociation rate constants for $Cd^{2+}$, e.g. $k_{1A} = k_{1B}$, $k_{2A} = k_{2B}$ etc., Eq. 5 and Eq. 6 simplify to:

$$\overline{\tau_2} = \frac{1}{k_{A1}}\left(1 + \frac{k_{A2}}{2k_{2A}}\right) = \frac{1}{k_{CC,10}^{app}} \quad \text{..... [7]}$$

$$\overline{\tau_1} = \frac{1}{2k_{1A}\left[Cd^{2+}\right]} = \frac{1}{k_{CC,01}^{app}\left[Cd^{2+}\right]} \quad \text{..... [8]}$$

Further, the overall dissociation equilibrium constant ($K_{d,CC}$) for the chelation of $Cd^{2+}$ is:

$$K_{d,CC} = \frac{k_{A1}k_{2A}}{k_{1A}k_{A2}} = K_{d,A}K_{d,2} \quad \text{..... [9]}$$

where $K_{d,A}$ (= $k_{A1}/k_{1A}$) and $K_{d,2}$ (= $k_{2A}/k_{A2}$) are the equilibrium dissociation constants of the first and second binding steps, respectively.

The apparent dissociation constant (Table 1) refers to the equilibrium between “inside” and “outside” the box (the low and high conductance states):

$$K_{d,CC}^{app} = \frac{\overline{\tau_1}\left[Cd^{2+}\right]}{\overline{\tau_2}} = \frac{k_{A1}k_{2A}}{k_{1A}\left(2k_{2A} + k_{A2}\right)}$$

$K^{app}_{d,CC}$ reduces to $K_{d,CC}$ if $k_{2A} << k_{A2}$.

By using Eq. 8, $k_{1A} = k^{app}_{CC,01}/2 = (2.7 \pm 0.9) \times 10^4\ M^{-1}s^{-1}$.

By using $k_{1A}$ and the value of $k_{Cd,10}$ for $P_C$ (Table 1) as $k_{A1}$:

$$K_{d,A} = k_{A1}/k_{1A} = (4.8 \pm 1.7) \times 10^{-4}\ M$$

By substituting the same value for $k_{A1}$ into Eq. 7 and using the apparent rate constant $k^{app}_{CC,10}$, we find:

$$K_{d,2} = k_{2A}/k_{A2} = (1.3 \pm 0.2) \times 10^{-3}$$

and the overall dissociation constant for 2, the fully coordinated $Cd^{2+}$ complex:

$$K_{d,CC} = (6.6 \pm 2.6) \times 10^{-7}\ M$$

The $K_{d,CC}$ value is similar to the apparent dissociation constant $K^{app}_{d,CC}$ for the same $P_{CC}$ pore (Table 1), and is over 300 times lower than $K_{d,Cd}$ for $P_C$, the pore containing a single cysteine. The lower overall dissociation constant for $P_{CC}$ is due to the stability of the complex when $Cd^{2+}$ is coordinated by both cysteines ($k_{2A} << k_{A2}$), and not by a higher association rate constant for $Cd^{2+}$.

## 4. Binding of $Cd^{2+}$ ion by $P_{HC}$

Noise analysis with the histidine-only mutant $P_H$, i.e. $(AG)_6(L135H\text{-}AG)_1$ (see Fig. S3), shows that $Cd^{2+}$ undergoes fast association and dissociation kinetics with the imidazole group. The residence time of $Cd^{2+}$ on $P_H$ is very short, hence the $P_H$-$Cd^{2+}$ complex is not represented by a distinct time-resolved current level. Therefore, $P_{HC}$ is analysed with H in the scheme below ($P_{HC}$ with $Cd^{2+}$ bound to His only) having the same conductance as the metal-free $P_{HC}$, 1. The observed binding events (Fig. 8*A*) presumably arise from the structures in the box:

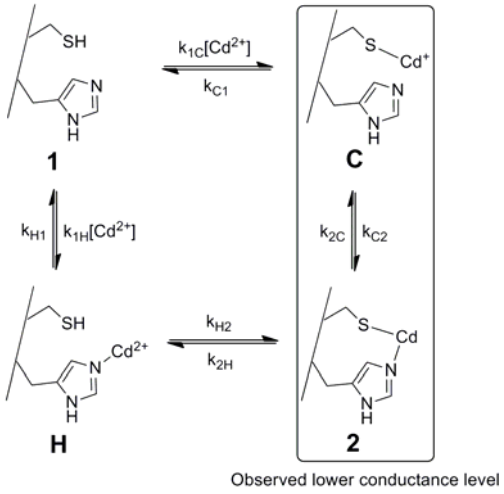


Our experimental results (Table 1 in the main text) show that 1) the association rate constant of $Cd^{2+}$ with $P_{HC}$ is 22-fold larger than that with $P_C$ and 2) the dissociation rate constants of $Cd^{2+}$ from $P_C$ and $P_{HC}$ are similar.

Considering the equilibrium in the box, the probabilities of finding C or 2 in the box are:

$$p_C = \frac{k_{2C}}{k_{2C} + k_{C2}} \quad \text{.....[10]}$$

$$p_2 = \frac{k_{C2}}{k_{2C} + k_{C2}} \quad \text{.....[11]}$$

such that $p_c + p_2 = 1$.

For moving out of the box, the apparent dissociation rate constant $k^{app}_{HC,10}$ (see Table 1):

$$k^{app}_{HC,10} = k_{C1}p_C + k_{2H}p_2$$

Substitution of Eq. 10 and Eq. 11 gives:

$$k^{app}_{HC,10} = \frac{k_{C1}k_{2C} + k_{2H}k_{C2}}{k_{2C} + k_{C2}} \quad \text{.....[12]}$$

The lifetime in the box is therefore:

$$\overline{\tau}_2 = \frac{1}{k^{app}_{HC,10}} = \frac{k_{2C} + k_{C2}}{k_{C1}k_{2C} + k_{2H}k_{C2}} \quad \text{.....[13]}$$

If $k_{2C} >> k_{C2}$ and $k_{C1}k_{2C} >> k_{2H}k_{C2}$, then $\overline{\tau}_2 = 1/k_{C1}$. If $k_{C2} >> k_{2C}$ and in the case that $k_{C1}k_{2C} << k_{2H}k_{C2}$, then $\overline{\tau}_2 = 1/k_{2H}$. The similar dissociation rate constants for $Cd^{2+}$ from $P_{HC}$ and $P_C$ (Table 1), suggest that the first case may operate, although $k_{2H}$ may, by coincidence, have similar value to the dissociation rate constant ($k_{Cd,10}$) of $P_C$.

Considering the two species outside the box, the probabilities of finding 1 and H are:

$$p_1 = \frac{k_{H1}}{\left(k_{H1} + k_{1H}\left[Cd^{2+}\right]\right)} \quad \text{.....[14]}$$

$$p_H = \frac{k_{1H}\left[Cd^{2+}\right]}{\left(k_{H1} + k_{1H}\left[Cd^{2+}\right]\right)} \quad \text{.....[15]}$$

such that $p_H + p_1 = 1$.

For moving into the box, the association rate $v_{assoc}$ is:

$$v_{assoc} = k_{1C}\left[Cd^{2+}\right]p_1 + k_{H2}p_H$$

Substituting Eq. 14 and Eq. 15 gives:

$$v_{assoc} = \frac{(k_{1C}k_{H1} + k_{H2}k_{1H})[Cd^{2+}]}{(k_{H1} + k_{1H}[Cd^{2+}])} \quad \text{.....[16]}$$

Therefore, the lifetime outside the box is:

$$\bar{\tau}_1 = \frac{1}{v_{assoc}} = \frac{k_{H1} + k_{1H}[Cd^{2+}])}{(k_{1C}k_{H1} + k_{H2}k_{1H})[Cd^{2+}]} \quad \text{.....[17]}$$

With our experimental values of $k_{H1} \sim k_{H,10} = (2.5 \pm 0.4) \times 10^4$ $s^{-1}$, $k_{1H} \sim k_{H,01} = (2.2 \pm 0.1) \times 10^6$ $M^{-1}s^{-1}$ (see Fig. S3) and the maximum $[Cd^{2+}] = 20$ μM, $k_{H1} >> k_{1H}[Cd^{2+}]$, and Eq. 17 can be simplified to:

$$\bar{\tau}_1 = \frac{1}{v_{assoc}} = \frac{k_{H1}}{(k_{1C}k_{H1} + k_{H2}k_{1H})[Cd^{2+}]} \quad \text{.....[18]}$$

which supports the observed first-order $[Cd^{2+}]$-dependence of $1/\bar{\tau}_1$ (represented by $1/\bar{\tau}_{PHC}$ in Fig. 8*B*).

So in the experimental $[Cd^{2+}]$ range of 5–20 μM, the apparent association rate is:

$$k^{app}_{HC,01} = \frac{(k_{1C}k_{H1} + k_{H2}k_{1H})}{k_{H1}} \quad \text{.....[19]}$$

In one limiting case, association is primarily to form C, i.e. $k_{1C}k_{H1} >> k_{1H}k_{H2}$, and $k^{app}_{HC,01} \sim k_{1C}$. Because $k^{app}_{HC,01} >> k_{Cd,01}$, if this case is operative the reactivity of the cysteine residue must be increased, presumably because the $pK_a$ value is lowered by the neighboring histidine, thereby increasing the fraction of the cysteine side-chain that is in the reactive thiolate form.

In a second limiting case, association is primarily to form 2, i.e. $k_{1C}k_{H1} << k_{1H}k_{H2}$, and $k^{app}_{HC,01} \sim k_{H2}(k_{1H}/k_{H1})$. Because $k_{1H}/k_{H1} \sim 88$ $M^{-1}$ (data in Fig. S3), $k_{H2} \sim 1.5 \times 10^4$ $s^{-1}$ for this pathway to be operative with the observed rate constant ($k^{app}_{HC,01} = (1.3 \pm 0.3) \times 10^6$ $M^{-1}s^{-1}$ (Table 1)). Because $k_{Cd,01} = (5.9 \pm 0.6) \times 10^4 M^{-1}s^{-1}$, the effective concentration of $Cd^{2+}$ in structure H is ~0.25 M.

The lowering of the $pK_a$ of Cys and the preassociation of $Cd^{2+}$ with His, cannot be distinguished with the current data. Of course, association cannot be

through say 2 and dissociation through C without recourse to "perpetual motion".

## 5. Binding of $Cd^{2+}$ ion to the histidine residue of $P_H$

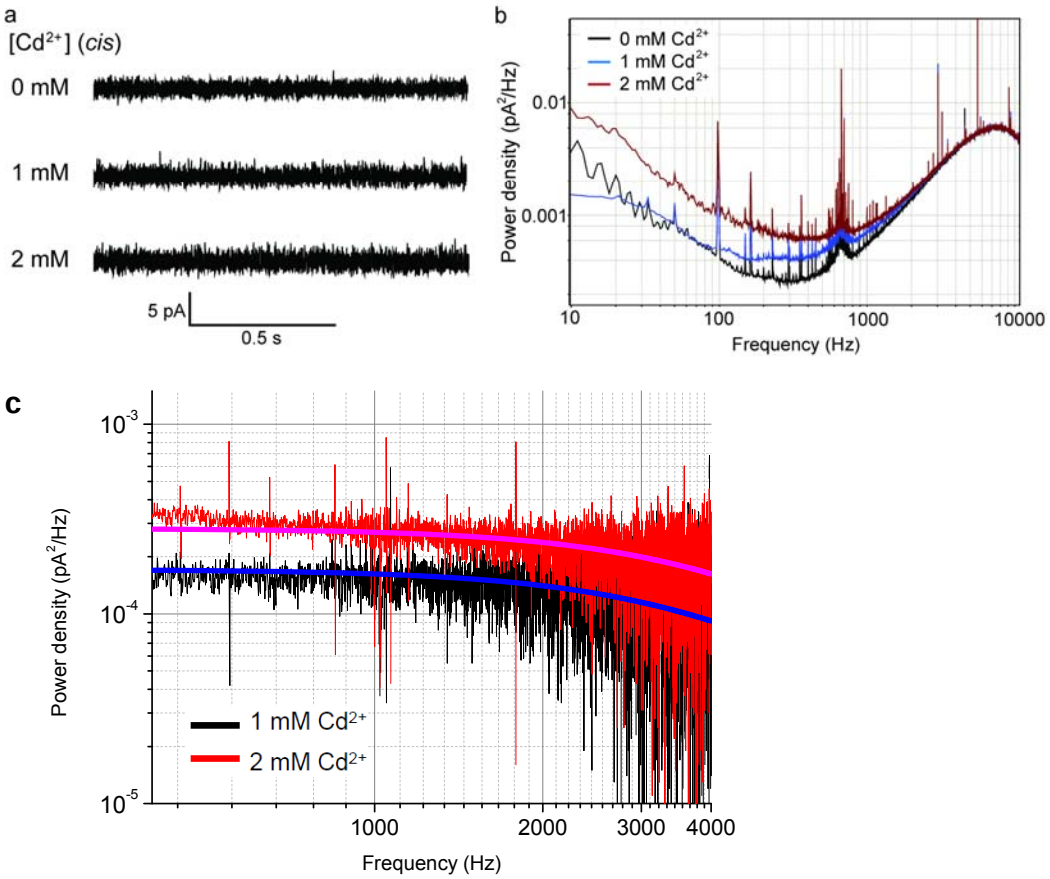


**Figure S3.** Reversible binding of $Cd^{2+}$ ion to $P_H$. (*A*) Stacked current recording traces of $(AG)_6(L135H\text{-}AG)_1$), $P_H$, at different concentrations of $Cd(NO_3)_2$ (*cis*). Experimental conditions were the same as in Fig. 5 of the main text. The traces were acquired with a low-pass 4-pole Bessel filter set at 10 kHz and acquired at 100 kHz. The excerpts shown are digitally low-pass filtered at 1000 Hz. The transient binding of $Cd^{2+}$ does not produce a new discrete current level, instead it increases the signal noise. (*B*) Current power spectra of the three traces shown in (*A*). (*C*) Current power spectra at 1 and 2 mM $Cd^{2+}$ after the subtraction of the background (no $Cd^{2+}$). The spectra are fitted to Lorentzian distributions, with the current blockade by $Cd^{2+}$ taken to be 4 pA, to obtain the association and dissociation rate constants of $Cd^{2+}$, and hence the equilibrium dissociation constant (7,8): $k_{H,01}$ = (2.2 ± 0.1) × $10^6$ $M^{-1}s^{-1}$; $k_{H,10}$ = (2.5 ± 0.4) × $10^4$ $s^{-1}$; $K_{d,H}$ = (1.1 ± 0.2) × $10^{-2}$ M (n = 2).

## SUPPORTING REFERENCES


1. Greenwood, N. N., and A. Earnshaw. 1984. Chemistry of the Elements; Permagon Press/New York. 1185–1187.
2. Nan, J., and X.-P. Yan. 2010. A circular dichroism probe for L-cysteine based on the self-assembly of chiral complex nanoparticles. Chem. Eur. J. 16:423–427.
3. Shen, J.-S., D.-H. Li, M.-B. Zhang, J. Zhou, H. Zhang, and Y.-B. Jiang. 2011. Metal−metal-interaction-facilitated coordination polymer as a sensing ensemble. Langmuir 27:481–486.
4. Shen, J.-S., D.-H. Li, Q.-G. Cai, and Y.-B. Jiang. 2009. Highly selective iodide-responsive gel-sol state transition in supramolecular hydrogels. J. Mater. Chem. 19:6219–6214.
5. Andersson, L.-O. 1972. Study of some silver-thiol complexes and polymers: stoichiometry and optical effects. J. Polym. Sci., Part A-1 10:1963–1973.
6. Colquhoun, D., and A. G. Hawkes. 2009. The principles of the stochastic interpretation of ion-channel mechanisms. In Single-channel recording. B. Sakmann, and E. Neher, editors. Springer/New York, London. 397–482.
7. DeFelice, L. J. 1981. Introduction to Membrane Noise. Plenum Press/New York. 296–313.
8. Verveen, A. A., and L. J. DeFelice. 1974. Membrane noise. Prog. Biophys. Mol. Biol. 28:189–265.